ANNULUS FLOW BEHAVIOR OF GELDART GROUP B PARTICLES IN A PILOT-SCALE CFB RISER

Aditya Anantharaman[1], Allan Issangya[2], S.B. Reddy Karri[2], John Findlay[2], Christine M. Hrenya[3], Ray A. Cocco[2], Jia Wei Chew[1,4,*]

[1]*School of Chemical and Biomedical Engineering, Nanyang Technological University, Singapore*

[2]*Particulate Solid Research Incorporated, Chicago, Illinois, U.S.A.*

[3]*Department of Chemical and Biological Engineering, University of Colorado at Boulder, Boulder, Colorado, U.S.A.*

[4]*Singapore Membrane Technology Centre, Nanyang Environment and Water Research Institute, Nanyang Technological University, Singapore*

*Email: *JChew@ntu.edu.sg*

Abstract – Solids flow direction near the wall of a CFB riser was studied for three monodisperse, two binary mixtures and one continuous particle size distribution (PSD) of Geldart Group B particles. Measurements were taken at five axial positions along a 0.3 m diameter, 18 m tall pilot-scale CFB riser at four operating conditions. The data were compared to predictions available from flow regime maps. Results showed that (i) for monodisperse systems, particle diameter was more dominant in dictating upflow annulus behavior; (ii) the binary mixtures exhibited largely upflow annulus behavior, presumably due to the dominant influence of the larger constituent particles in dictating upflow annulus behavior; (iii) for the continuous particle size distribution (PSD), the impact of this type of polydispersity was more pronounced at lower solids loading conditions; and (iv) the applicability of the available regime maps, which were largely developed based on Geldart Group A particles, was found to be limited for the Geldart Group B and non-monodisperse particle systems investigated in this study.

INTRODUCTION

Gas-solid circulating fluidized beds (CFBs) have wide-ranging industrial applications (Fan and Zhu, 1998; Grace et al., 2003), including fluid catalytic cracking (FCC), chemical synthesis, coal gasification and more recently chemical looping. Despite the widespread usage, gaps in the knowledge base persist, one of which is the annulus flow behavior in the riser, which is the focus of this study. In particular, core-annulus flow (i.e., a dilute upflow core and a dense downflow annulus) in a CFB riser of Geldart Group A (Geldart, 1973) particles is well-acknowledged. The core-annulus phenomenon was first proposed by Bierl and Gajdos (1982). They proposed a flow structure, which consisted of a dilute core of upward moving particles, which occupied most of the cross-section, and a relatively dense annulus at the riser wall, which consisted mainly of downward-moving solids. Weinstein et al. (1986) also acknowledged the core-annulus structure for describing the radial solids distribution in a CFB.

Most of the literature describes the core-annulus structure as a radially segregated solids flow with a lean core consisting of upflowing particles and a thin dense annulus consisting of downflowing particles. However, in the case of dense phase flow, a core–annular solids distribution persists, but, instead of a downflow annulus, an upflow annulus was consistently observed (Bi and Zhou, 1993; Issangya, 1998; Issangya et al., 1997a; Issangya et al., 1997b; Karri and Knowlton, 1991; Schuurmans, 1980). Bai et al. (1999) found that the statistical and chaotic analyses from the signals obtained from such high-density CFB (HDCFB) risers were markedly different from in the ones from more dilute CFB risers. Gupta and Berruti (1998) demarcated 'dense phase flow' and 'fast fluidization' by an empirical correlation developed from experimental data on Geldart Group A particles. Grace et al. (1999) subsequently proposed a new flow regime, using experimental data obtained mostly from Geldart Group A particles. They called it 'Dense Suspension Upflow' (DSU). The key feature of the DSU regime is an upflow annulus, while retaining the variation of radial solids concentration as in a conventional core-annulus flow (i.e., dilute core and dense annulus). Issangya et al. (2000) further carried out measurements of local voidage in an HDCFB riser using Geldart Group A particles and found that, while voidage fluctuations were low at the core, they reached a peak value (i.e., maximum heterogeneity) at some distance away from the wall, which is in contrast with the conventional core-annulus flow whereby maximum heterogeneity was found at the wall. Subsequently, Kim et al. (2004) demarcated three different flow regimes for CFB risers, based on the flow direction of the annulus and the solids holdup across the riser cross-section

at a given height. They used previously published experimental data, most of which was from Geldart Group A particles. Many authors have investigated the 'Dense Suspension Upflow' (DSU) regime (Geng et al., 2013; Geng et al., 2014; Parssinen and Zhu, 2001; Wang et al., 2014; Wei et al., 1998), but with the focus largely on Geldart group A. Although there has been some research on demarcating flow regimes in CFB risers containing Geldart Group B particles (Das et al., 2008), none has focused on investigating the core-annulus behavior of these systems. Geldart Group B particles are well-acknowledged to fluidize differently from Geldart Group A particles, with the most significant difference being the lack of cohesion in the former (Geldart, 1973). In particular, a previous study has shown surprisingly that Geldart Group B particles exhibited a reverse core-annulus behavior (i.e., a dense core and a dilute annulus) due to the higher Stokes numbers (St) of the particles (Chew et al., 2012c). Because behavioral trends of Geldart Group A particles cannot be directly extrapolated to predict those of Group B, an investigation into the hydrodynamics of the latter warranted especially with the increasing prominence in its use as inert materials to improve the fluidization quality of biomass (Cui and Grace, 2007; Oliveira et al., 2013; Paudel and Feng, 2013). Accordingly, this study is focused on understanding the annulus flow behavior of Geldart Group B particles.

The lack of knowledge on the impact of polydispersity, which is an ever-present aspect of solids processing in industry, has been flagged as being a critical gap to bridge (Curtis and van Wachem, 2004; Hrenya, 2010; Muzzio et al., 2002; Sundaresan, 2001). Polydisperse systems have been shown to exhibit distinctly different behaviors from monodisperse systems (Chew et al., 2011a; Fan et al., 1990; Hrenya, 2010; Ottino and Khakhar, 2000; Rowe and Nienow, 1976; van Ommen et al., 2011). Distinctly different behaviors among monodisperse systems and different types of polydispersity (e.g., binary mixtures and continuous particle size distributions (PSDs)) have been reported in bubbling fluidized beds (Chew and Hrenya, 2011; Chew et al., 2010; Hoffmann and Romp, 1991; Lin et al., 2002; van Ommen et al., 2011) and circulating fluidized beds (CFBs) (Cahyadi et al., 2015; Chew et al., 2015; Chew et al., 2013; Issangya et al., 2010). The impact of polydispersity on the annulus flow behavior has, however, not been studied.

The present work aims to experimentally study the annulus flow behavior of Geldart group B particles in a pilot-scale CFB riser. Six particle systems, namely, three monodisperse, two binary, and one continuous PSD, were studied at four operating conditions. Measurements were done at five axial positions along the riser. The annulus flow behavior was compared to the available flow regime maps (Bi and Grace, 1995; Grace et al., 1999; Gupta and Berruti, 1998; Kim et al., 2004).

EXPERIMENTAL

Fig. 1 shows a schematic of the circulating fluidized bed (CFB) unit located at Particulate Solid Research, Incorporated (PSRI) in Chicago, USA. The component of focus is the riser, which had an inner diameter (ID) of 0.3 m and was 18.3 m tall. The air and solids first passed through a mixing pot located at the bottom of the riser. The mixing pot was a chamber where solids from the standpipe and air from the blowers were introduced and allowed to mix, to ensure a uniform distribution of air and solids as they entered the riser. The rounded-elbow riser exit had the same ID as the riser, and was connected downstream to two cyclones in series. The mass flux of the solids was controlled by a pneumatic slide valve. The fluidizing air was supplied by Atlas Copco blowers. The inlet air temperature and relative humidity were measured with an Omega HX93AV-RP1 humidity probe inserted flush with the wall before the mixing pot. The air flow rate was determined from measurements across an orifice plate installed in the air supply line.

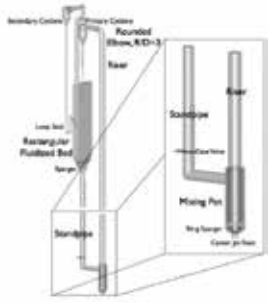

Fig. 1. Schematic of the pilot-scale circulating fluidized bed (CFB)

Six particle systems, all belonging to Geldart Group B, were investigated: three monodisperse systems, with two among them having different particle diameters (d_{ave}) and two among them having different particle densities (ρ_p); two binary mixtures, one consisting of consitutents differing in d_{ave} (i.e., binary-size) and one consisting of constituents differing in ρ_p (i.e., binary-density); and a continuous particle size distribution (PSD). All particles were approximately spherical. Table 1 lists the particle systems investigated and the relevant properties.

Table 1. Properties of the materials investigated

System Type	PSD Width, σ/d_{ave} (%)	Material	Volume %	Average particle diameter, d_{ave} (µm)	Particle density, ρ_p (kg/m^3)
Monodisperse	12	Small glass	100	170	2500
Monodisperse	9	Large glass	100	650	2500
Monodisperse	11	HDPE	100	650	900
Binary-size	12	Small glass	50	170	2500
	9	Large glass	50	650	2500
Binary-density	9	Large glass	50	650	2500
	11	HDPE	50	650	900
Continuous PSD	25	Small glass	100	170	2500

In the case of monodisperse materials, small glass (ρ_p = 2500 kg/m^3 and d_{ave} = 170 µm), large glass (ρ_p = 2500 kg/m^3 and d_{ave} = 650 µm) and high density polyethylene, HDPE (ρ_p = 900 kg/m^3 and d_{ave} = 650 µm), were investigated. While small glass and large glass had the same ρ_p but different d_{ave}, large glass and HDPE had the same d_{ave} but different ρ_p. As it was not experimentally possible to obtain identically sized particles, efforts were made to obtain as narrow a size distribution as possible. Glass beads of both sizes from Midwest Finishing Systems and HDPE from Dyneon LLC were sieved using a Sweco industrial sieve. The PSD widths, defined as the ratio of the standard deviation (σ) of mass-based PSD to d_{ave}, of monodisperse small glass, large glass and HDPE were 12%, 9% and 11%, respectively, as listed in Table 1. Binary mixtures were prepared by mixing two monodisperse materials in a one-to-one volume ratio, while the continuous PSD (σ/d_{ave} = 25 %) was used as obtained from the vendor.

The operating conditions investigated were selected with considerations of the test unit constraints, as detailed elsewhere (Chew et al., 2011a; Chew et al., 2012c). Tests for all the six particle systems were conducted at two superficial gas velocities (U_g) and two mass fluxes (G_s) in the riser as given in Table 3. The superficial gas velocity (U_g) values were determined by an orifice plate (as mentioned in Section 2.1), while the overall mass flux (G_s) was calculated by summing up the local mass flux measurements via an extraction probe (as will be detailed in Section 2.4). The inlet temperature of the gas was in the range of 15 – 25 °C, while the pressure profiles have been reported in a previous study (Chew et al., 2012c). The solids loading ratio (m), a dimensionless quantity defined as the ratio of overall mass flux to gas mass flux, is also given in Table 2.

Table 2: Operating conditions for the different materials

Material	Superficial gas velocity, U_g (m/s)	Mass flux, G_s (kg/m^{2}s)	Solids loading ratio, m (-)
Monodisperse materials and binary mixtures	13.5	120	7.4
	13.5	260	16.0
	17.0	120	5.9
	17.0	260	12.7
Continuous PSD	10.0	50	4.2
	10.0	300	25.0
	15.0	50	2.8
	15.0	300	16.7

The method of measuring the local mass flux in the riser has been detailed elsewhere (Chew et al., 2011b). In brief, the upward and downward local mass flux values ($G_{r,upward}$ and $G_{r,downward}$, respectively) at a given radial location were measured using an extraction probe. The extraction probe was operated non-isokinetically (Aguillón et al., 1995; Chew et al., 2011b; Rhodes and Laussmann, 1992; Salvaterra et al., 2005; Zhang et al., 1997), and it was verified that the suction velocity did not affect the results, which is expected of Geldart Group B particles as they tend not to follow gas streamlines due to the relatively higher Stokes number (Chew et al., 2011b, 2012c). Probe measurements were validated by conducting repeated runs for different durations, and the error associated with the overall mass flux (G_s) was determined to be within an acceptable tolerance of ±10% between repeated measurements and along the riser height. Interested readers are referred elsewhere (Chew et al., 2011a) for details. To allow for easier comparison across the different G_s conditions, the local mass flux was normalized with respect to the overall mass flux (G_s), which is expressed as follows (Chew et al., 2011b):

$$G_{r,net,norm} = \frac{G_{r,upward} - G_{r,downward}}{G_s} \quad (1)$$

whereby G_s is the summation of the net flux measured at 11 radial positions across the riser, as detailed in a previous study (Chew et al., 2011b).

Because this study only focuses on annulus flow behavior, only the $G_{r,net,norm}$ values at r/R = 0.94 (where r is the radial position assessed and R is the radius of the riser), which is the radial position closest to the wall where the measurement was taken, were taken into account.

ANNULUS MASS FLUX PROFILES

In view of the focus of this study on understanding annulus flow behavior, only the mass flux near the wall was investigated. Specifically, this analysis was targeted at identifying the operating conditions, riser axial positions and particle properties (i.e., material type, polydispersity type) at which the particle systems examined exhibited upflow (i.e., positive $G_{r,net,norm}$) or downflow (i.e., negative $G_{r,net,norm}$) annulus behavior. The development of a regime map was beyond the scope of this study, but instead the current data was juxtaposed onto the available regime maps to gauge the applicability or lack thereof to Geldart Group B particles.

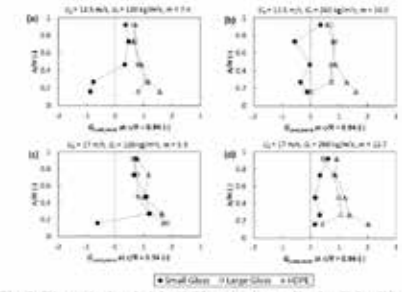

Fig. 2. Dimensionless height (h/H) versus normalized radial solids flux ($G_{r,net,norm}$) at r/R = 0.94 for three monodisperse particle types at four operating conditions: (a) U_g = 13.5 m/s, G_s = 120 kg/m²s, m = 7.4; (b) U_g = 13.5 m/s, G_s = 260 kg/m²s, m = 16.0; (c) U_g = 17 m/s, G_s = 120 kg/m²s, m = 5.9; and (d) U_g = 17 m/s, G_s = 260 kg/m²s, m = 12.7. Note that negative and positive $G_{r,net,norm}$ values represent respectively downflow and upflow annulus.

The effect of the particle properties of monodisperse small and large glass, and HDPE particles on the annulus is showed in Fig. 2. Normalized riser axial position, h/H (where h is the height evaluated and H is the total height of the riser), is plotted against the normalized radial solids flux, $G_{r,net,norm}$, at r/R = 0.94. The properties of the large glass, small glass and HDPE particles are given in Table 2. Each sub-plot represents a given operating condition (Table 3). Each error bar represents the span of values obtained from at least two repeat measurements, although the error bars are largely too small due to the normalization to be clearly noticeable. A negative $G_{r,net,norm}$ value means downflowing of solids in the annulus, while a positive $G_{r,net,norm}$ value means upflowing of solids in the annulus. Four observations from Fig. 2 are worth highlighting. Firstly, regarding the solids flow direction in the annulus, the larger glass and HDPE particles exhibited an upflow annulus at all operating conditions, whereas the smaller glass particles gave both an upflow and a downflow annulus behavior. This suggests that particle diameter (d_{ave}) rather than particle density (ρ_p) played a more dominant role in dictating upflow annulus behavior. Secondly, regarding the effect of particle density (ρ_p), the $G_{r,net,norm}$ values of the large glass and HDPE were largely similar, except at h/H = 0.16 for the higher G_s conditions (Figs. 2b and d), which implies that the variations in annulus behavior due to particle density were minimal higher up in the riser. Thirdly, regarding the effect of particle diameter, the $G_{r,net,norm}$ values of small glass and large glass were similar higher up in the riser ($h/H \geq 0.47$) at lower G_s conditions (Figs. 2a and c), and similar at the lowermost (h/H = 0.16) and uppermost (h/H = 0.92) heights of the riser at the higher G_s conditions (Figs. 2b and d). This reflects that the impact of particle diameter on annulus flow behavior was significant lower in the riser at lower G_s conditions and middle of the riser at higher G_s conditions. Fourthly, the $G_{r,net,norm}$ values of the three particle types were consistently similar across the operating conditions tested only at the highest h/H of 0.92, which presumably indicates the dominance of exit effects (Chew et al., 2012c; De Wilde et al., 2003; Gupta and Berruti, 2000; Pugsley et al., 1997; van der Meer et al., 2000) relative to particle property or operating condition. Fifthly, regarding axial variation of the annulus flow, the acceleration effects lower in the riser are clear, as indicated by the greater axial variation lower in the riser and the relatively invariant profiles above mid-height of the riser. In particular, the small glass exhibited the greatest axial variation at the lower G_s conditions, which suggests that the annulus flow of the small glass

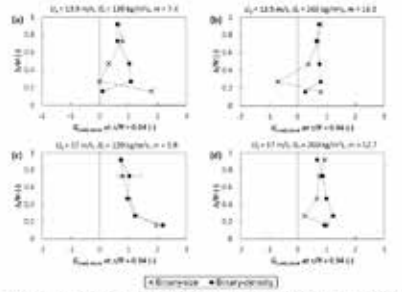

Fig. 3. Dimensionless height (h/H) versus normalized radial solids flux ($G_{r,net,norm}$) at r/R = 0.94 for the two binary mixtures at four operating conditions: (a) U_g = 13.5 m/s, G_s = 120 kg/m²s, m = 7.4; (b) U_g = 13.5 m/s, G_s = 260 kg/m²s, m = 16.0; (c) U_g = 17 m/s, G_s = 120 kg/m²s, m = 5.9; and (d) U_g = 17 m/s, G_s = 260 kg/m²s, m = 12.7.

was more affected by the acceleration effects at these conditions than the larger particles. It should be noted that the acceleration-deceleration and/or entrance-exit effects along the riser were more influential on the mass flux (Chew et al., 2011b) and cluster (Chew et al., 2012a, b) trends characterized for the same riser, materials and operating conditions, where the impact of axial position was the most dominant (relative to material properties and/or operating conditions).

Analogous to Fig. 2, Fig. 3 plots h/H versus $G_{r,net,norm}$ values at $r/R = 0.94$ for the binary-size and binary-density particle mixtures (Table 2). The common constituent in these mixtures was the large glass particle constituent. Four observations can be made. Firstly, both binary mixtures exhibited an upflow annulus, except for the binary-size mixture at $h/H = 0.27$ at the lower U_g conditions (Figs. 3a and b). This indicates that the larger constituent in the binary-size mixture dominated in dictating the upflow annulus behavior. Secondly, the $G_{r,net,norm}$ values for the two mixtures were similar throughout the riser at the lowest solid loading condition (Fig. 3c), indicating minimal impact of particle properties at this condition, which is consistent with Fig. 2c. Thirdly, the two mixtures each exhibited similar $G_{r,net,norm}$ trends with respect to h/H under the three higher solid loading conditions (Figs. 3a, b and d), which implies a negligible impact of operating conditions. Fourthly, the difference in $G_{r,net,norm}$ values between the mixtures were minimal higher up in the riser ($h/H \geq 0.73$) at all operating conditions, which indicate the dominating influence of riser position over particle property or operating condition. This is similar to that in Fig. 2 except that it was restricted only to $h/H = 0.92$.

Fig. 4 illustrates h/H versus $G_{r,net,norm}$ at $r/R = 0.94$ for the continuous particle size distribution (PSD) of the small glass particles at $U_g = 10$ and 15 m/s and $G_s = 50$ and 300 kg/m^{2}s. The four tests had solids loadings of 2.8, 4.2, 16.7 and 25.0. Comparing the lower G_s conditions (Figs. 6a and c), it can be seen that the tendency for an upflow annulus was greater at higher U_g (Fig. 6c). Similarly, for the higher G_s conditions (Figs. 6b and d) too, the tendency for an upflow annulus increased with increasing U_g, though to a relatively lesser extent than that at the lower G_s conditions. This suggests that, for continuous PSDs, superficial gas velocity (U_g) was the more dominant factor than overall solids mass flux in dictating upflow annulus behavior.

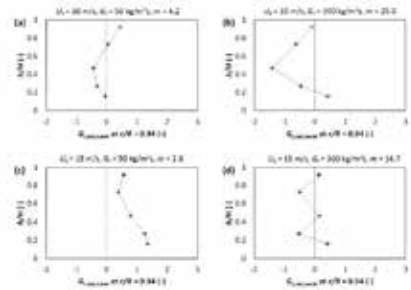

Fig. 4. Dimensionless height (h/H) versus normalized radial solids flux ($G_{r,net,norm}$) at $r/R = 0.94$ for the continuous PSD of small glass at four operating conditions: (a) $U_g = 10$ m/s, $G_s = 50$ kg/m^{2}s, $m = 4.2$; (b) $U_g = 10$ m/s, $G_s = 300$ kg/m^{2}s, $m = 25.0$; (c) $U_g = 15$ m/s, $G_s = 50$ kg/m^{2}s, $m = 2.8$; and (d) $U_g = 15$ m/s, $G_s = 300$ kg/m^{2}s, $m = 16.7$.

It is reasonable to infer the impact of the continuous PSD vis-à-vis the monodisperse small glass systems by comparing (i) Fig. 2b ($m = 16$) with Fig. 6d ($m = 16.7$), and (ii) Fig. 2c ($m = 5.9$) with Fig. 6a ($m = 4.2$), each pair of which is at nearly similar solid loadings. Regarding (i), the $G_{r,net,norm}$ trends were very similar both in terms of magnitude and variation with respect to h/H, which indicates the presence of a continuous PSD did not change the annulus flow behavior at $m \approx 16$. However, at the lower m condition assessed in (ii), the monodisperse small glass exhibited distinct upflow annulus behavior at $h/H \geq 0.27$ (Fig. 2c), whereas the continuous PSD exhibited a clear upflow annulus behavior only at $h/H = 0.92$ (Fig. 6a), which suggests that the impact of continuous PSD was significant at lower solids loading (m) conditions. More specifically for the continuous PSD of small glass in Fig. 6, the highest solid loading ($m = 25.0$) condition (Fig. 6b) gave the most marked downflow annulus behavior in terms of the most negative $G_{r,net,norm}$ value at $h/H = 0.47$, while the lowest solid loading ($m = 2.8$) condition (Fig. 6c) exhibited upflow annulus throughout the riser. It is worth pointing out that the radial mass flux profile for the continuous PSD of small glass was observed to be distinctly different at the lowest m condition relative to the other three conditions, which was different from the trends for the monodisperse small glass system, and was attributed either to behavioral differences due to polydispersity or the wider range of operating conditions (Chew et al., 2011b).

REGIME MAPS

A regime map of CFB riser flow to demarcate conditions whereby core-annulus flow prevails was developed by Bi and Grace (1995). Three principal regimes were identified in order of decreasing superficial gas velocity (U_g), namely, homogeneous dilute-phase flow, core-annulus flow and fast fluidization. The homogeneous dilute-phase flow regime was described as having minimal lateral variation of solid concentration, with

uniform upflow across the entire cross-section. The core-annulus flow regime, was delineated as having a lean upflow core and a denser downflow annulus. The fast fluidization regime was described as having a significant axial variation of solid concentration, with a dense, turbulent bottom and a core-annulus top. The transition between the homogeneous dilute-phase flow and core-annulus regimes, defined as the minimum pressure velocity, V_{mp}, was presented (Bi and Fan, 1991) as:

$$V_{mp} = 10.1\left(g d_p\right)^{0.347}\left(\frac{G_s}{\rho_g}\right)^{0.31}\left(\frac{d_{ave}}{D}\right)^{-0.139}\mathrm{Ar}^{-0.021} \tag{2}$$

$$\mathrm{Ar} = \frac{\rho_g(\rho_p-\rho_g)g d_{ave}^3}{\mu_g^2} \tag{3}$$

where μ_g is gas viscosity (1.81×10^{-5} Pa.s). As for the superficial velocity delineating the core-annulus and fast fluidization regimes, a type A choking velocity, V_{ca}, was defined (Bi and Fan, 1991) as:

$$V_{ca} = 21.6\sqrt{g d_{ave}}\mathrm{Ar}^{0.105}\left(\frac{G_s}{\rho_g V_{ca}}\right)^{0.542} \tag{4}$$

Specifically, type A choking velocity is the superficial gas velocity below which particles accumulate at the riser bottom.

The regime map was developed largely based on data for Geldart Group A particles (Bi and Grace, 1995). This study was aimed at assessing if the regime map is applicable to the Geldart Group B particles investigated. Fig. 5 presents data from the current work as discrete data points plotted on the regime map demarcated by V_{mp} (Eq. 2) and V_{ca} (Eq. 4) (Bi and Grace, 1995). The x-axis represents the ratio of the overall solids flux to particle density, G_s/ρ_p, while the y-axis the superficial gas velocity, U_g. Because V_{ca} and V_{mp} change with material properties, the three monodisperse particles (Figs. 5a - c), the two binary mixtures (Figs. 5d– e) and the continuous PSD (Fig. 5f) of small glass are plotted separately. The average particle diameter and density for the monodisperse materials and the continuous PSD are given in Table 2. The properties for the binary mixtures were calculated as the arithmetic averages of the constituents. Each discrete data point represents the predicted annulus flow behavior of a particle system at a specific operating condition. The filled or bold markers represent cases whereby a mixture of upflow and downflow annulus flows was experimentally observed along the riser, while the empty or regular markers represent cases of solely upflow annulus throughout the riser.

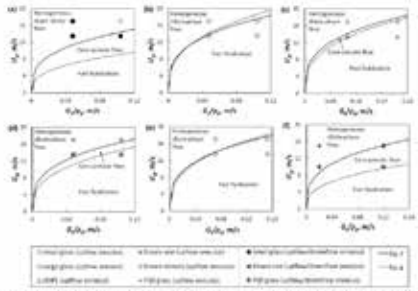

Fig. 5. Comparison of experimental data with prediction of flow regime map of Bi and Grace (1995) for (a) small glass, (b) large glass, (c) HDPE, (d) binary-size mixture, (e) binary-density mixture, and (f) continuous PSD of small glass. The solid and dotted lines represent V_{mp} (Eq. 2) and V_{ca} (Eq. 4) respectively. 'Homogeneous dilute-phase flow' represents upflow annulus with minimal lateral variation of solids concentration, 'Core-annulus flow' represents a dense downflow annulus and lean upflow core, and 'Fast fluidization' represents a dense turbulent bottom and core-annulus top.

Three observations are worth noting in Fig. 5. Firstly, although none of the three regimes of Bi and Grace (1995) account for upflow annulus, the upflow annulus behaviors observed in the current study are scattered among the regimes. Secondly, the regime map interestingly predicts that the core-annulus regime with downflow annulus is almost non-existent in the cases of large glass (Fig. 5b), large HDPE (Fig. 5c) and binary-density mixture (Fig. 5e). Whereas all three particle systems consistently exhibited an upflow annulus regardless of operating conditions, the regime map shows contradictorily that the fast fluidization regime would be present for the higher G_s conditions and the homogeneous dilute-phase flow regime for the lowest m condition. Thirdly, only one data point, which corresponds to the highest solid loading, m, each in monodisperse small glass (Fig. 5a) and continuous PSD of small glass (Fig. 5f), falls into the core-annulus regime, although both particle systems exhibited a mixture of upflow and downflow annulus at different axial positions along the riser. Fig. 5 hence appears to indicate the inadequacy of the regime map developed for Geldart Group A particles to be applied for Geldart Group B systems.

Grace et al. (1999) subsequently accounted for upflow annulus behavior through the introduction of a new regime called 'dense suspension upflow' (DSU). The DSU regime was reported to have core-annulus flow with upflow annulus, and solid volume fraction (ϕ) ≥ 0.07. A semi-empirical correlation was developed to distinguish between conventional core-annulus flow with downflow annulus, termed in the new regime map as 'fast fluidization', and the new DSU regime. The threshold Reynolds number for DSU, $\mathrm{Re}_{\mathrm{DSU}}$, and the Archimedes number, Ar, were correlated to give (Grace et al., 1999):

$$\mathrm{Re}_{\mathrm{DSU}} = 0.113\left(\frac{G_s d_{ave}}{\mu_g}\right)^{1.192} \mathrm{Ar}^{-0.064} \quad (5)$$

Analogously, Gupta and Berruti (1998) had published a correlation to distinguish between 'fast fluidization' and 'dense phase flow' (DPF) regimes. The DPF is similar to DSU in that it requires a core-annulus flow with upflow annulus, but the conditions differ from DSU in that the solids flux has to be greater than 100 kg/m^{2}s and $\phi > 0.15$. The Gupta and Berruti (1998) semi-empirical correlation is expressed as follows

$$\mathrm{Re}_{\mathrm{DPF}} = 12.55\left(\frac{G_s}{v_t \rho_p}\right)^{0.55} \mathrm{Ar}^{0.36} \quad (6)$$

where $\mathrm{Re}_{\mathrm{DPF}}$ is the threshold Reynolds number for dense phase flow (DPF), and v_t is the particle terminal velocity.

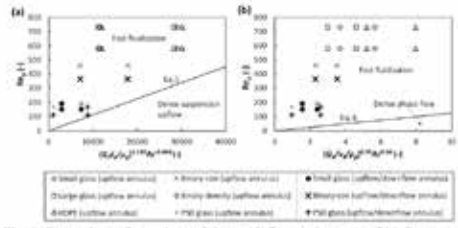

Fig. 6. Comparison of experimental data with flow regime map of (a) Grace et al. (1999) and (b) Gupta and Berruti (1998). The solid lines represent Eqs. 5 and 6 in (a) and (b), respectively. Note that 'Fast fluidization' represents a dense downflow annulus and lean upflow core (which is unlike Fig. 7), while 'Dense suspension upflow' and 'Dense phase flow' both represent upflow annulus.

Fig. 6 presents the regime maps of Grace et al. (1999) (Fig. 6a) and Gupta and Berruti (1998) (Fig. 6b). The *x*-axes represent dimensionless groups which are functions of G_s and Ar, and the *y*-axes represent the particle Reynolds number, Re_p. The lines demarcating the regimes are given by Eqs. 5 and 6 in Figs. 6a and b, respectively. Similar to Fig. 5, each discrete data point represents the predicted annulus flow behavior of a particle system at a specific operating condition, and the filled or bold markers represent cases whereby a mixture of upflow and downflow annulus flows was experimentally observed along the riser, while the empty or regular markers represent cases of solely upflow annulus throughout the riser. Fig. 6 illustrates that, although upflow annulus was observed in most of the cases in this study, all the data points fall in the 'fast fluidization' regime (which has a downflow annulus behavior) and none in the DSU or DPF regimes (which predict upflow annulus behavior). Interestingly, the large glass, large HDPE and binary-density systems, which consistently exhibited upflow annulus behavior, are furthest from the DSU and DPF regimes on the regime maps (Fig. 6). Therefore, even though the upflow annulus behavior was found in Geldart Group A particle systems, the new regime maps could not account for upflow annulus in CFB risers of Geldart Group B particles.

REFERENCES

Aguillón, J., Shakourzadeh, K., Guigon, P., 1995. Comparative study of non-isokinetic sampling probes for solids flux measurement in circulating fluidized beds. Powder Technology 83, 79-84.

Bai, D., Issangya, A., Grace, J.R., 1999. Characteristics of Gas-Fluidized Beds in Different Flow Regimes. Industrial & Engineering Chemistry Research 38, 803-811.

Bi, H.T., Fan, L.S., 1991. Regime transitions in gas-solid circulating fluidized beds, AIChE Annual Meeting, , Los Angeles.

Bi, H.T., Grace, J.R., 1995. Flow regime diagrams for gas-solid fluidization and upward transport. International Journal of Multiphase Flow 21, 1229-1236.

Bi, H.T., Zhou, J., 1993. Static Instability Analysis of Circulating Fluidized Beds and Concept of High-Density Risers. AIChE Journal 39, 1272-1280.

Bierl, T.W., Gajdos, L.T., 1982. Phenomenological modelling of reaction experiments in risers. Final Report, DOE/MC-14249-1149. Environmental Research and Technology, Inc.

Cahyadi, A., Chew, J.W., Hrenya, C.M., Cocco, R.A., 2015. Comparative study of Transport Disengaging Height (TDH) correlations in gas–solid fluidization. Powder Technology 275, 220-238.

Chew, J.W., Cahyadi, A., Hrenya, C.M., Cocco, R., 2015. Review of entrainment correlations in gas-solid fluidization. Chemical Engineering Journal 260, 152-171.

Chew, J.W., Hays, R., Findlay, J.G., Karri, S.B.R., Knowlton, T.M., Cocco, R.A., Hrenya, C.M., 2011a. Species segregation of binary mixtures and a continuous size distribution of Group B particles in riser flow. Chemical Engineering Science 66, 4595-4604.

Chew, J.W., Hays, R., Findlay, J.G., Knowlton, T.M., Karri, S.B.R., Cocco, R.A., Hrenya, C.M., 2011b. Impact of material property and operating conditions on mass flux profiles of monodisperse and polydisperse Group B particles in a CFB riser. Powder Technology 214, 89-98.

Chew, J.W., Hays, R., Findlay, J.G., Knowlton, T.M., Karri, S.B.R., Cocco, R.A., Hrenya, C.M., 2012a. Cluster characteristics of Geldart Group B particles in a pilot-scale CFB riser. I. Monodisperse systems. Chemical Engineering Science 68, 72-81.

Chew, J.W., Hays, R., Findlay, J.G., Knowlton, T.M., Karri, S.B.R., Cocco, R.A., Hrenya, C.M., 2012b. Cluster characteristics of Geldart Group B particles in a pilot-scale CFB riser. II. Polydisperse systems. Chemical Engineering Science 68, 82-93.
Chew, J.W., Hays, R., Findlay, J.G., Knowlton, T.M., Karri, S.B.R., Cocco, R.A., Hrenya, C.M., 2012c. Reverse core-annular flow of Geldart Group B particles in risers. Powder Technology 221, 1-12.
Chew, J.W., Hrenya, C.M., 2011. Link between bubbling and segregation patterns in gas-fluidized beds with continuous size distributions. AIChE Journal 57, 3003-3011.
Chew, J.W., Parker, D.M., Hrenya, C.M., 2013. Elutriation and species segregation characteristics of polydisperse mixtures of Group B particles in a dilute CFB riser. AIChE Journal 59, 84-95.
Chew, J.W., Wolz, J.R., Hrenya, C.M., 2010. Axial segregation in bubbling gas-fluidized beds with gaussian and lognormal distributions of Geldart Group B particles. AIChE Journal 56, 3049-3061.
Cui, H., Grace, J.R., 2007. Fluidization of biomass particles: A review of experimental multiphase flow aspects. Chemical Engineering Science 62, 45-55.
Curtis, J.S., van Wachem, B., 2004. Modeling particle-laden flows: A research outlook. AIChE Journal 50, 2638-2645.
Das, M., Bandyopadhyay, A., Meikap, B.C., Saha, R.K., 2008. Axial voidage profiles and identification of flow regimes in the riser of a circulating fluidized bed. Chemical Engineering Journal 145, 249-258.
De Wilde, J., Marin, G.B., Heynderickx, G.J., 2003. The effects of abrupt T-outlets in a riser: 3D simulation using the kinetic theory of granular flow. Chemical Engineering Science 58, 877-885.
Fan, L.S., Zhu, C., 1998. Principles of Gas-Solid Flows. Cambridge University Press, Cambridge, New York, pp. 421-460.
Fan, L.T., Chen, Y.M., Lai, F.S., 1990. Recent developments in solids mixing. Powder Technology 61, 255-287.
Geldart, D., 1973. Types of gas fluidization. Powder Technology 7, 285-292.
Geng, Q., Zhu, X., Liu, Y., Liu, Y., Li, C., You, X., 2013. Gas–solid flow behavior and contact efficiency in a circulating-turbulent fluidized bed. Powder Technology 245, 134-145.
Geng, Q., Zhu, X., Yang, J., You, X., Liu, Y., Li, C., 2014. Flow regime identification in a novel circulating-turbulent fluidized bed. Chemical Engineering Journal 244, 493-504.
Grace, J.R., Bi, H., Golriz, M., 2003. Circulating Fluidized Beds, in: Yang, W.C. (Ed.), Handbook of Fluidization and Fluid-Particle Systems. Marcel Dekker, New York.
Grace, J.R., Issangya, A., Bai, D., Bi, H., 1999. Situating the High-Density Circulating Fluidized Bed. AIChE Journal 45, 2108-2116.
Gupta, S.K., Berruti, F., 1998. Modeling considerations for large scale high density risers, in: Fan, L.S., Knowlton, T. (Eds.), Fluidization IX. Engineering Foundation, New York, pp. 189-194.
Gupta, S.K., Berruti, F., 2000. Evaluation of the gas-solid suspension density in CFB risers with exit effects. Powder Technology 108, 21-31.
Hoffmann, A.C., Romp, E.J., 1991. Segregation in a fluidized powder of a continuous size distribution. Powder Technology 66, 119-126.
Hrenya, C.M., 2010. Kinetic Theory for Granular Materials: Polydispersity, in: Pannala, S., Syamlal, M., O'Brien, T. (Eds.), Computational Gas-Solids Flows and Reacting Systems: Theory, Methods, and Practice. IGI Global, Hershey, PA, pp. 102-127.
Issangya, A., 1998. Flow dynamics in high density circulating fluidized beds, PhD dissertation. University of British Columbia, Vancouver, British Columbia, Canada.
Issangya, A., Bai, D., Bi, H.T., Lim, K.S., Zhu, J., Grace, J.R., 1997a. Axial Solids Holdup Profiles in a High-Density Circulating Fluidized Bed Riser, in: Kwauk, M., Li, J. (Eds.), Circulating Fluidized Bed Technology V. Science Press, Beijing, p. 60.
Issangya, A., Bai, D., Grace, J.R., Lim, K.S., Zhu, J., 1997b. Flow Behavior in the Riser of a High-Density Circulating Fluidized Bed. AiChE Symposium Series 93, 25-30.
Issangya, A., Grace, J.R., Bai, D., Zhu, J., 2000. Further measurements of flow dynamics in a high-density circulating fluidized bed riser. Powder Technology 111, 104-113.
Issangya, A., Karri, S.B.R., Knowlton, T., 2010. Effects Of Imposed Solids Flux And Pressure On Gas Bypassing In Deep Fluidized Beds Of Group A Materials, in: Kim, S.D., Kang, Y., Lee, J.K., Seo, Y.C. (Eds.), The 13th International Conference on Fluidization - New Paradigm in Fluidization Engineering. ECI Symposium Series, pp. 1-10.
Karri, S.B.R., Knowlton, T., 1991. A Practical Definition of the Fast Fluidization Regime, in: Basu, P., Horio, M., Hasatani, M. (Eds.), Circulating Fluidized Bed Technology III. Pergamon Press, Oxford, p. 67.
Kim, S.W., Kirbas, G., Bi, H., Lim, C.J., Grace, J.R., 2004. Flow behavior and regime transition in a high-density circulating fluidized bed riser. Chemical Engineering Science 59, 3955-3963.
Lin, C.L., Wey, M.Y., You, S.D., 2002. The effect of particle size distribution on minimum fluidization velocity at high temperature. Powder Technology 126, 297-301.

Muzzio, F.J., Shinbrot, T., Glasser, B.J., 2002. Powder technology in the pharmaceutical industry: The need to catch up fast. Powder Technology 124, 1-7.
Oliveira, T.J.P., Cardoso, C.R., Ataíde, C.H., 2013. Bubbling fluidization of biomass and sand binary mixtures: Minimum fluidization velocity and particle segregation. Chemical Engineering and Processing: Process Intensification 72, 113-121.
Ottino, J.M., Khakhar, D.V., 2000. Mixing and segregation of granular materials. Annual Review of Fluid Mechanics 32, 55-91.
Parssinen, J.H., Zhu, J.X., 2001. Particle velocity and flow development in a long and high-flux circulating fluidized bed riser. Chemical Engineering Science 56, 5295-5303.
Paudel, B., Feng, Z.-G., 2013. Prediction of minimum fluidization velocity for binary mixtures of biomass and inert particles. Powder Technology 237, 134-140.
Pugsley, T., Lapointe, D., Hirschberg, B., Werther, J., 1997. Exit effects in circulating fluidized bed risers. Canadian Journal of Chemical Engineering 75, 1001-1010.
Rhodes, M.J., Laussmann, P., 1992. Characterizing non-uniformities in gas-particle flow in the riser of a circulating fluidized bed. Powder Technology 72, 277-284.
Rowe, P.N., Nienow, A.W., 1976. Particle mixing and segregation in gas-fluidized beds - review. Powder Technology 15, 141-147.
Salvaterra, A., Geldart, D., Ocone, R., 2005. Solid Flux in a Circulating Fluidized Bed Riser. Chemical Engineering Research and Design 83, 24-29.
Schuurmans, H.J.A., 1980. Measurements in a Commercial Catalytic Cracking Unit. Industrial & Engineering Chemistry Process Design and Development 19, 267-271.
Sundaresan, S., 2001. Some outstanding questions in handling of cohesionless particles. Powder Technology 115, 2-7.
van der Meer, E.H., Thorpe, R.B., Davidson, J.F., 2000. Flow patterns in the square cross-section riser of a circulating fluidised bed and the effect of riser exit design. Chemical Engineering Science 55, 4079-4099.
van Ommen, J.R., Sasic, S., van der Schaaf, J., Gheorghiu, S., Johnsson, F., Coppens, M.O., 2011. Time-series analysis of pressure fluctuations in gas-solid fluidized beds - A review. International Journal of Multiphase Flow 37, 403-428.
Wang, C., Zhu, J., Li, C., Barghi, S., 2014. Detailed measurements of particle velocity and solids flux in a high density circulating fluidized bed riser. Chemical Engineering Science 114, 9-20.
Wei, F., Lin, H., Cheng, Y., Wang, Z., Jin, Y., 1998. Profiles of particle velocity and solids fraction in a high-density riser. Powder Technology 100, 183-189.
Weinstein, H., Shao, M., Schnitzlein, M., 1986. RADIAL VARIATION IN SOLID DENSITY IN HIGH VELOCITY FLUIDIZATION in: Basu, P. (Ed.), Circulating Fluidized Bed Technology. Pergamon, Oxford, pp. 201-206.
Zhang, W., Johnsson, F., Leckner, B., 1997. Momentum probe and sampling probe for measurement of particle flow properties in CFB boilers. Chemical Engineering Science 52, 497-509.